NIH Public Access
Author Manuscript
Biomaterials. Author manuscript; available in PMC 2007 September 20.

Published in final edited form as:
Biomaterials. 2007 January ; 28(3): 459–467.

Segmental Bone Regeneration Using a Load Bearing Biodegradable Carrier of Bone Morphogenetic Protein-2

Tien-Min G. Chu[1,2,*], **Stuart J. Warden**[3], **Charles H. Turner**[1,2], and **Rena L. Stewart**[2]

1 *Department of Biomedical Engineering, Purdue School of Engineering and Technology, Indiana University-Purdue University Indianapolis, Indianapolis, IN 46202*

2 *Department of Orthopaedic Surgery, Indiana University School of Medicine, Indianapolis, IN. 46202*

3 *Department of Physical Therapy, School of Health and Rehabilitation Sciences, Indiana University, Indianapolis, IN. 46202*

Abstract

Segmental defect regeneration has been a clinical challenge. Current tissue engineering approach using porous biodegradable scaffolds to delivery osteogenic cells and growth factors demonstrated success in facilitating bone regeneration in these cases. However, due to the lack of mechanical property, the porous scaffolds were evaluated in non-load bearing area or were stabilized with stress-shielding devices (bone plate or external fixation). In this paper, we tested a scaffold that does not require a bone plate because it has sufficient biomechanical strength. The tube-shaped scaffolds were manufactured from poly(propylene) fumarate/tricalcium phosphate (PPF/TCP) composites. Dicalcium phosphate dehydrate (DCPD) were used as bone morphogenetic protein -2 (BMP-2) carrier. Twenty two scaffolds were implanted in 5 mm segmental defects in rat femurs stabilized with k-wire for 6 and 15 weeks with and without 10 μg of rhBMP-2. Bridging of the segmental defect was evaluated first radiographically and was confirmed by histology and micro- computer tomography (μ-CT) imaging. The scaffolds in the BMP group maintained the bone length throughout the duration of the study and allow for bridging. The scaffolds in the control group failed to induce bridging and collapsed at 15 weeks. Peripheral computed tomography (pQCT) showed that BMP-2 does not increase the bone mineral density in the callus. Finally, the scaffold in BMP group was found to restore the mechanical property of the rat femur after 15 weeks. Our results demonstrated that the load-bearing BMP-2 scaffold can maintain bone length and allow successfully regeneration in segmental defects.

INTRODUCTION

Segmental bone defects resulting from trauma or pathology represent a common and significant clinical problem. Limb amputation was historically the principal treatment option for these defects as they typically do not heal spontaneously [1]. With advances in medicine and science, alternative treatment options have developed such as the use of bone grafting techniques. Autologous bone grafts are preferred as they possess inherent osteoconductivity, osteogenicity and osteoinductivity. However, there is often limited supply of suitable bone for autologous grafting, and its collection is frequently associated with donor-site morbidity. An alternative is to use allogeneic bone grafts from donors or cadavers. These circumvent some of the

*Corresponding author. Tel./fax: +1-317-278-8716 Email address: tgchu@iupui.edu (T. Chu)

Publisher's Disclaimer: This is a PDF file of an unedited manuscript that has been accepted for publication. As a service to our customers we are providing this early version of the manuscript. The manuscript will undergo copyediting, typesetting, and review of the resulting proof before it is published in its final citable form. Please note that during the production process errors may be discovered which could affect the content, and all legal disclaimers that apply to the journal pertain.

NIH-PA Author Manuscript
NIH-PA Author Manuscript
NIH-PA Author Manuscript

NIH-PA Author Manuscript

NIH-PA Author Manuscript

NIH-PA Author Manuscript

limitations associated with harvesting autologous grafts, but allogeneic bone grafts lack osteogenicity, have limited osteoinductivity and present a risk of disease transmission. These limitations necessitate the pursuit of alternatives for the management of segmental bone defects, with the latest approach being to use tissue engineering techniques.

Tissue engineering for bone typically involves coupling osteogenic cells and/or osteoinductive growth factors with osteoconductive scaffolds [2,3] In terms of osteoinductive growth factors, most research has focused on the use of the bone morphogenic proteins (BMPs) and, in particular, BMP-2 [1,4–8]. BMP-2 is a bone matrix protein that stimulates mesenchymal cell chemotaxis and proliferation, and promotes the differentiation of these cells into chondrocytes and osteoblasts [6,8]. These cellular effects bestow BMP-2 potent osteoinductive capabilities, which are primarily evident by the induction of new bone formation via a process of endochondral ossification when implanted at ectopic sites [9,10]. This osteoinductive action of BMP-2 is well established to be beneficial during the repair of fractures and segmental bone defects [1,5,7,8].

BMP-2 induces bone regeneration following injury and has been approved for limited clinical use in the form of recombinant human BMP-2 (rhBMP-2) [5]. However, rhBMP application has been limited by ongoing delivery issues. To facilitate retention of rhBMP-2 at the treatment site and reduce the effective dose, an appropriate carrier is required [9]. The preferred carrier consists of a scaffold that is both biocompatible and bioresorbable in order to limit tissue rejection and exposure to the scaffold material, respectively [11]. While numerous scaffolds have been manufactured that meet these requirements [12] many lack the ability to tolerate appreciable loads. This is of importance as segmental defects frequently occur in load bearing bones. Scaffolds need to be able to tolerate loading so that patient morbidity is minimized during reparation and the structure of the engineered bone is optimized to the local mechanical environment. Few load bearing scaffolds have been described in the literature, with many studies of tissue engineered bone regeneration with BMP-2 being conducted at non-load bearing sites [13–16] or in defects stabilized with stress-shielding devices (bone plates or external fixation) [17–20].

In the current paper, we present a tissue engineering strategy for bone regeneration using rhBMP-2 carried by a novel load bearing biodegradable scaffold. Tube shaped scaffolds were fabricated from a high strength biodegradable composite and calcium phosphate cement, and implanted into critical sized defects in an established rodent model [21]. Defects and scaffolds were stabilized with a load-sharing device (intramedullary pin). The aim was to investigate the effect of our novel load bearing scaffold carrying rhBMP-2 on segmental defect repair in the rat femur.

MATERIALS AND METHODS

Animals

Twenty-two adult male Long-Evans rats (weight = 450–550 g) were purchased from Charles River Laboratory (Wilmington, MA) and acclimatized for a minimum of one week prior to experimentation. Animals had *ad libitum* access to standard rat chow and water at all times, and all procedures were performed with prior approval of the Institutional Animal Care and Use Committee of Indiana University.

Scaffold manufacture

Polypropylene fumarate (PPF) with a molecular weight of 1750 g/mol and PI = 1.5 was obtained from Prof. Antonios Mikos (Rice University, Houston, TX). A thermal-curable PPF/tricalcium phosphate (TCP) suspension was prepared by mixing PPF, N-vinyl pyroolidinone

NIH-PA Author Manuscript

NIH-PA Author Manuscript

NIH-PA Author Manuscript

(NVP), and TCP at a weight ratio of 1:0.75:0.66 [22]. Tube shaped structures (outer diameter = 4 mm, inner diameter = 2 mm, height = 5 mm, with four side holes of 800 μm diameter) were created by the indirect casting technique developed by Chu et al [23,24]. Briefly, a scaffold design was generated using commercial Computer-Aided-Design software and a negative model obtained by using Boolean computer operation. Wax casting-molds were fabricated on a 3-D Inkjet Printing Machine (T66, Solidscape Inc. NH) according to the model design. The PPF/TCP slurry was combined with 0.5% benzoyl peroxide (thermal initiator) and 10 μl of dimethyl p-toluidine (accelerator), and cast into the wax mold. Following polymerization, the wax mold was removed by acetone to reveal the scaffold. rhBMP-2 was aseptically added to half of the scaffolds prior to surgery by adding 10 μg of rhBMP-2 (Wyeth, Cambridge, MA) to porous dicalcium phosphate dihydrate (DCPD) cement previously packed into the side holes of the scaffold (BMP-2 group). In the remaining scaffolds, DCPD without rhBMP-2 was added to the side holes (control group).

Segmental defect induction and surgical implantation of the scaffolds

All animals underwent surgery to create a unilateral midshaft femur segmental defect into which either a rhBMP-containing scaffold (BMP group) or control scaffold (control group) was implanted. A non-scaffold control group was not used in this study since the non-healing nature of 5 mm segmental defects in the rat femur is well established [25,26]. Following a pre-operative subcutaneous dose of buprenorphine hydrochloride analgesia (0.05 mg/kg; Buprenex®— Reckitt Benckiser Pharmaceuticals Ltd, Inc, Richmond, VA), surgical anesthesia was achieved using a mixture of ketamine (60–80 mg/kg; Ketaset®—Fort Dodge Animal Health, Fort Dodge, IA) and xylazine (7.5 mg/kg; Sedazine®—Fort Dodge Animal Health, Fort Dodge, IA) introduced intraperitoneally. The fur was clipped and cleaned using alternating chlorhexidine and 70% ethanol scrubs. Using a sterile technique, a 30-mm longitudinal incision was made over the lateral thigh, beginning just distal to the lateral knee joint and extending proximally. The intermuscular septum between the vastus lateralis and hamstring muscles was divided using blunt dissection to localize the femur. The lateral structures stabilizing the patella were divided and the patella manually dislocated medially. A 5 mm segment of the midshaft femur was removed following two parallel osteotomies under irrigation using a Dremel drill (Robert Bosch Tool Corporation, Mount Prospect IL) with attached diamond-embedded wafer blade (Super Flex Diamond Disc, Miltex Inc, York, PA). To stabilize the fracture, a 1.25 mm diameter stainless steel K-wire (Synthes Inc, West Chester, PA) was inserted retrograde into the distal intramedullary canal, beginning in the knee between the femoral condyles. The wire was advanced to the segment defect and a scaffold centered over the tip. The wire passed through the central canal of the scaffold and was further advanced in a retrograde fashion into the proximal intramedullary canal and through the greater trochanter (Fig. 1). The distal tip of the wire was cut flush with the femoral condyles. After thorough irrigation, the patella was relocated and stabilized with an absorbable suture, and the muscle and skin layers closed and sutured.

Radiographic analysis

In vivo X-rays were taken of eight rats (n = 4/group) at one, three, six, 12 and 15 weeks post-operatively using a portable x-ray machine (AMX-110, GE Corp, Waukesha, WI). The rats were anesthetized using isoflurane (Abbott Laboratories, North Chicago, IL) and placed prone on an X-ray film cassette 29 inches beneath the X-ray source. Exposure was at 60 kVp for 2.5 mAs. All films were evaluated in a blinded fashion by three independent evaluators using a three point radiographic scoring system (0 = no callus formation; 1 = possible union across the gap; 2 = complete callus bridging across the gap).

NIH-PA Author Manuscript

NIH-PA Author Manuscript

NIH-PA Author Manuscript

Assessment time points and specimen preparation

Animals were killed at six (n = 4/group) and 15 (n = 7/group) weeks postoperatively by inhalation of carbon dioxide followed by bilateral pneuothorax. In four rats per group, both femora were dissected free, and prepared for microcomputed tomography (μCT), peripheral quantitative computed tomography (pQCT) and histological assessment by fixing in 10% neutral buffered formalin for 48 h and storing in 70% alcohol. In the remaining six rats in the 15 week group, hind limbs were prepared for mechanical testing by wrapping in gauze and storing in normal saline at −4°C.

Microcomputed tomography

μCT was performed on a randomly selected subgroup of segmental defects to visualize in three dimensions the stage of healing at six and 15 weeks post-operatively. The intramedullary K-wires were carefully removed before further assessment as metal causes beam-hardening artifacts during quantitative radiographic imaging. Each femur was centered in the gantry of a desktop μCT machine (μCT-20; Scanco Medical AG, Bassersdorf, Switzerland) and scanned at 50 kVp / 32 keV (160 μA) with an isotropic voxel size of 8 μm. The scanned slices were reconstructed to show in three dimensions the external and cut-away views of the reparative callus and scaffold.

Peripheral quantitative computed tomography

pQCT was used to assess callus and scaffold volumetric bone mineral density (vBMD; mg/cm^3) at six and 15 weeks post-operatively. Each femur was centered in the gantry of a pQCT machine (XCT Research SA+; Stratec Medizintechnik, Pforzheim, Germany) and scanned with a 70 μm voxel size. Five 0.46 mm cross-sectional slices were scanned at 1 mm intervals, with the center slice coinciding with the center of the scaffold. Contouring mode 1 with a threshold of 240 mg/cm^3 was used to separate bone from soft tissue. Areas containing only the callus or scaffold were selected from the images using the region-of-interest (ROI) tool function, and the vBMD of the callus and scaffolds were determined, respectively.

Histological assessment

Femurs were processed for histomorphometry by washing, dehydrating in graded alcohols, and infiltrating and embedding undecalcified in methyl methacrylate (Aldrich Chemical Co., Inc., Milwaukee, WI). Thin (7 μm) sections were taken through the long axis of each femur in the sagittal plane using a rotating microtome (Reichert-Jung 2050; Reichert-Jung, Heidelberg, Germany). Alternating sections were stained with hematoxyline-and-eosin and McNeals tetrachrome. Sections were viewed on Nikon Optiphot fluorescence microscope (Nikon, Inc., Garden City, NJ).

Mechanical testing

For mechanical testing, femurs were brought to room temperature overnight in a saline bath, the gauze wrapping removed, soft-tissue dissected free and the intramedullary pin carefully removed. A custom-made four-point bending fixture with a span width of 22.0 mm between the lower contacts and 8.0 mm between the upper contacts was used. The femurs were positioned cranial side up across the lower contacts. A preload of 1.0 N and crosshead speed of 20.0 mm/min were used to break the femurs. Measurements made using force-versus-displacement curves included: ultimate force (N) or the height of the curve, stiffness (N/mm) or the maximum slope of the curve, and energy to ultimate force (mJ) or the area under the curve up to ultimate force.

NIH-PA Author Manuscript

NIH-PA Author Manuscript

NIH-PA Author Manuscript

Statistical analyses

Statistical analyses were performed with the Statistical Package for Social Sciences (SPSS 6.1.1; Norusis/SPSS Inc., Chicago, IL) software. All comparisons were two-tailed with a level of significance set at 0.05, unless otherwise indicated. Mann-Whitney U-tests were used to compare radiographic scores between scaffold groups (BMP vs. control) at each time point. vBMD was compared by two-way factorial analyses of variance (ANOVA), with scaffold group (BMP vs. control) and time since surgery (six vs. 15 weeks) being the independent variables. Mechanical properties were compared by two-way, one-repeated measure ANOVA, with scaffold group (BMP vs. control) and surgical group (segmental defect vs. intact control) being the between- and within-animal independent variables, respectively. Paired or unpaired t-tests were performed in the event of a significant ANOVA interaction, with a Bonferroni correction to the level significance for the number of pair-wise comparisons. ANOVA main effects were explored in the event of a non-significant interaction. Surgical group effect sizes were assessed using mean percentage differences and their 95% confidence intervals (CIs) between femurs with segmental defects and contra-lateral intact control femurs, whereas time since surgery effect sizes were determined using mean differences and their 95% CI between six and 15 weeks.

RESULTS

Radiographic analysis

Qualitative assessment of the x-rays films showed no bone formation in any specimen at 1 week after surgery. At 3 weeks, continuous callus had formed and bridged across the gap defect in two of the four rats in the BMP group. In the control group, some cortical bone thickening and callus formation was noticed immediately adjacent to the scaffold; however, callus did not bridge the gap. At 6 weeks, the callus bridge in the BMP group showed signs of consolidation and further thickening of the cortex next to the scaffold. In the control group, isolated radiopaque spots were noticed (islands of bone formation), but callus bridging was not present. Further thickening and remodeling of the callus was seen at 12 and 15 weeks in the BMP groups. AT 12 and 15 weeks the control group showed increased callus size in the area adjacent to the scaffold, but there was no x-ray evidence of bridging callus (Fig. 2). In the x-ray score, all rats in the BMP group showed a score of 0 at week 1. Three rats received scores of 1 and 2 at week 3. At six weeks, all rats received a score of 2. All rats in the control group received a score of 0 till 12 weeks. One rat received a score of 1 at 15 weeks (Table 1).

There were no significant differences on radiographic scoring between the BMP and control groups after one ($p = 1.00$) or three ($p = 0.11$) weeks. After six, 12 and 15 weeks, defects in the BMP group had significantly greater radiographic scores than those in the control group (all $p = 0.03$), indicating that the former had more advanced healing.

Histology

Histology sections at 6 weeks showed mineralized callus bridging the gap in the BMP group. Normal trabeculae were found between the periosteal callus and the scaffold (Fig. 3A). Residual DCPD can be seen in the side holes (Fig. 3B). Under H&E stain, normal fatty bone marrow was restored at 6 weeks (not shown). No inflammation reaction was seen in either BMP group or control group. In the control group, the histology showed characteristics of psuedoarthrosis with cartilage forming at the junction between the scaffold and the bone end. The periosteal callus did not bridge the gap (Fig. 3C). The histology of the BMP group at 15 weeks showed mature trabeculae between the scaffold and the periosteal callus (Fig. 3D). In the control group, the gap was filled with fibrous tissue and the scaffolds started to crumble (not shown).

NIH-PA Author Manuscript

NIH-PA Author Manuscript

NIH-PA Author Manuscript

Micro-CT analysis

Micro-CT scans showed continuous callus formation around the scaffold in the BMP group at 6 weeks. Bone has also formed inside the marrow cavity next to the intramedullary pin (pin removed prior to scanning). Normal trabecular bone was found between the cortical layer of the callus and the BMP group scaffolds. In contrast, the control group at 6 weeks shows minimal bone formation outside the scaffold and the callus did not bridge the gap. At 15 weeks, the bridging callus and the trabeculae between the scaffold and the cortex of the callus is evident in the BMP group (Fig. 4).

The histology and μCT results confirms the radiographic finding that defects in the BMP group to be bridged with mineralized callus that was integrated with the scaffold.

p-QCT analysis

At 6 weeks, the measured vBMD of the callus for the BMP group and the control group was 724.05 ± 108.71 mg/cm^3 and 742.00 ± 54.46 mg/cm^3, respectively. At 15 weeks, the vBMD of the callus increased to 959.06 ± 81.47 mg/cm^3 and 894.66 ± 59.82 mg/cm^3 for BMP group and control group. The measured vBMD in the native femur was 920.95 ± 49.53 mg/cm^3.

The mineral density of the scaffold was measured to evaluate the in vivo absorption of tricalcium phosphate in the scaffold. The mineral density of the scaffolds after 6 weeks of implantation in vivo was 625.96 ± 26.14 mg/cm^3 in the BMP group and 613.59 ± 16.35 mg/cm^3 in the control group. After 15 weeks of implantation in vivo, the mineral density of scaffold was 579.42 ± 13.99 mg/cm^3 in the BMP group and 574.82 ± 37.50 mg/cm^3 in the control group.

There were no significant interactions between group (BMP vs. control) and time since surgery (six vs. 15 weeks) on either callus ($p = 0.28$) or scaffold ($p = 0.79$) vBMD (Figure 4). Similarly, there were no group main effects on either callus ($p = 0.36$) or scaffold ($p = 0.62$) vBMD. In contrast, there were significant main effects for time since surgery on both callus ($p < 0.001$) and scaffold ($p < 0.01$) vBMD. Callus vBMD was 26% greater (mean difference = 193.2 mg/cm^3, 95% CI = 118.2 mg/cm^3 to 268.2 mg/cm^3) and scaffold vBMD was 6.9% lower (mean difference = −42.4 mg/cm^3, 95% CI = −65.7 mg/cm^3 to −19.1 mg/cm^3) at 15 weeks post-surgery than at six weeks (Figure 5).

Mechanical property results

Mechanical properties of the femurs were only measured at 15 weeks. There were significant interactions between scaffold group (BMP vs. control) and surgical group (segmental defect vs. intact control) on ultimate force (p =0.01) and stiffness ($p < 0.05$), but not energy to ultimate force ($p = 0.10$) (Figure 6). Segmental defects in the BMP group had 290%, 286% and 234% greater ultimate force ($p < 0.01$), stiffness ($p = 0.04$) and energy to ultimate force ($p = 0.02$) than segmental defects in the control group, respectively (Figure 6). There were no side-to-side differences in ultimate force (%diff = −1.4%, 95% CI = −35.7% to 32.8%), stiffness (%diff = −15.5%, 95% CI = −68.5% to 37.6%) or energy to ultimate force (%diff = −11.7%, 95% CI = −28.8% to 5.3%) in the BMP group between femurs with segmental defects and contra-lateral, intact control femurs (all $p = 0.15$ to 0.64). In contrast, femurs with segmental defects in the control group had lower ultimate force (%diff = −66.1%, 95% CI = −105.8% to −26.5%) and stiffness (%diff = −62.6%, 95% CI = −96.6% to −28.5%) than contra-lateral, intact control femurs (all $p < 0.02$). Energy to ultimate force between femurs with segmental defects and contra-lateral, intact control femurs did not differ in the control group (%diff = −61.4%, 95% CI = −126.4% to 3.6%) ($p = 0.06$).

NIH-PA Author Manuscript

NIH-PA Author Manuscript

NIH-PA Author Manuscript

DISCUSSION

We have shown that scaffold made from high strength biodegradable composite can be used as BMP2 carrier to facilitate segmental defect regeneration in partial load bearing condition, such as in the intramedullary pin fixation. This is clinically relevant since intramedullary pin fixation is commonly used for segmental defect fixation. In a retrospective study of ten patients treated for large bone defects, six of the ten treatments involve the use of intramedullary pins [27]. In another retrospective study, six of the seven patients treated for acute segmental defects involve the use of intramedullary pins [28]. In research, Tiyapatanaputi et al [29] demonstrated the use of pin to stabilize autograft, isograft and allograft in rat femoral defect model and found that the fixation using K-wire as intramedullary pin provided reproducible results in stabilized structural allograft. However, studies using intramedullary pin for stabilization tissue engineering scaffolds has been lacking.

In this paper, we stabilized the PPF/TCP tissue engineering scaffold by a 1.25 mm k-wire as intramedullary pin. This is a load-sharing model since the loads are shared by the friction between the intramedullary pin and the contact areas in the medullary canal and by the scaffolds. All BMP groups show bridging callus, indicating a stable biomechanical environment conducive to the formation of callus. Our previous experience showed that the scaffolds made from DCPD by itself (compressive strength = 0.5 MPa) collapsed one day after implantation, indicating that the rats bear load on the scaffolds (unpublished results). The PPF/TCP scaffold has an initial compressive strength of 23 MPa, but gradually reduces to 12 MPa after 12 weeks of incubation in phosphate buffered solution at 37°C [30]. The fact that PPF/TCP scaffold did not collapse during implantation indicates that the initial strength of the scaffold is sufficient to sustain the femoral loading in the rat model. When callus bridging failed to occur, the PPF/TCP scaffolds eventually collapsed after 15 weeks demonstrating that the degraded compressive strength of PPF/TCP at 15 weeks is no longer sufficient to support rat locomotor loads. This result together with the fact that the scaffold in the BMP group is still intact at 15 weeks also indicates that the bridging callus in the BMP group has assumed loading sharing/bearing function in the defect.

DCPD is biodegradable and has been used as BMP-2 carrier [25]. In this study, a dose of 10 μg of BMP-2 was found to induce callus formation, similar to the results by Ohura et al [25] and Yasko et al [26]. PPF/TCP is biodegradable [31], though very slowly, as pQCT measurements demonstrated that the scaffold density was reduced by less than 10% in 15 weeks of implantation. The long effect of the degradation byproduct on tissue is critical and will need to be studied in the future. Nonetheless, this study established that a compressive strength of 23 MPa will provide sufficient strength to withstand the initial load placed on the scaffold when the scaffold is implanted in rat femoral gap stabilized with intramedullary pin.

In BMP group and control group, we and found no difference in callus vBMD, in consistent with the findings by Hyun et al [32] where bone density in BMP-2 induced new bone was the same as normal bone. From our results, we conclude that it is the quantity and the distribution of the callus, but not the bone mineral density, that makes the difference between the BMP group and the control group.

CONCLUSIONS

In this study investigated a tissue engineering strategy for bone regeneration using BMP-2 carried by a load bearing biodegradable scaffold. We found that critical-sized segmental defects in the rodent femur have advanced radiological, histological and mechanical healing using our tissue engineering strategy of load-bearing scaffold stabilized with intramedullary pins. Radiographical and histological healing is enhanced with weight bearing biodegradable

NIH-PA Author Manuscript

NIH-PA Author Manuscript

NIH-PA Author Manuscript

scaffolds of rhBMP-2. The weight bearing biodegradable scaffold of BMP-2 do not influence the callus mineral density. Finally, the mechanical properties of the segmental defects are restored with weight bearing biodegradable scaffolds of BMP-2

Acknowledgements

The authors would like to thank Prof. Antonio Mikos for providing the poly(propylene fumarate) used in this study. The authors would also like to thank Wyeth Co. for providing the rhBMP-2. The research was supported by NIH EB005426.

References

1. Giannoudis PV, Pountos I. Tissue regeneration. The past, the present and the future. Injury 2005;36 (Suppl 4):S2–5. [PubMed: 16288758]
2. Buma P, Schreurs W, Verdonschot N. Skeletal tissue engineering-from in vitro studies to large animal models. Biomaterials 2004;25(9):1487–95. [PubMed: 14697851]
3. Mistry AS, Mikos AG. Tissue engineering strategies for bone regeneration. Adv Biochem Eng Biotechnol 2005;94:1–22. [PubMed: 15915866]
4. Cowan CM, Soo C, Ting K, Wu B. Evolving concepts in bone tissue engineering. Curr Top Dev Biol 2005;66:239–85. [PubMed: 15797456]
5. Mont, MA.; Ragland, PS.; Biggins, B.; Friedlaender, G.; Patel, T.; Cook, S., et al. J Bone Joint Surg Am. 86-A. 2004. Use of bone morphogenetic proteins for musculoskeletal applications. An overview; p. 41-55.
6. Reddi AH. Role of morphogenetic proteins in skeletal tissue engineering and regeneration. Nat Biotechnol 1998;16(3):247–52. [PubMed: 9528003]
7. Termaat MF, Den Boer FC, Bakker FC, Patka P, Haarman HJ. Bone morphogenetic proteins. Development and clinical efficacy in the treatment of fractures and bone defects. J Bone Joint Surg Am 2005;87(6):1367–78. [PubMed: 15930551]
8. Wozney JM, Rosen V. Bone morphogenetic protein and bone morphogenetic protein gene family in bone formation and repair. Clin Orthop Relat Res 1998;(346):26–37. [PubMed: 9577407]
9. Urist MR, Lietze A, Dawson E. Beta-tricalcium phosphate delivery system for bone morphogenetic protein. Clin Orthop Relat Res 1984;(187):277–80. [PubMed: 6744730]
10. Wang EA, Rosen V, D'Alessandro JS, Bauduy M, Cordes P, Harada T, et al. Recombinant human bone morphogenetic protein induces bone formation. Proc Natl Acad Sci U S A 1990;87(6):2220–4. [PubMed: 2315314]
11. Seeherman H, Wozney JM. Delivery of bone morphogenetic proteins for orthopedic tissue regeneration. Cytokine Growth Factor Rev 2005;16(3):329–45. [PubMed: 15936978]
12. Perry CR. Bone repair techniques, bone graft, and bone graft substitutes. Clin Orthop Relat Res 1999; (360):71–86. [PubMed: 10101312]
13. Akamaru T, Suh D, Boden SD, Kim HS, Minamide A, Louis-Ugbo J. Simple carrier matrix modifications can enhance delivery of recombinant human bone morphogenetic protein-2 for posterolateral spine fusion. Spine 2003;28(5):429–34. [PubMed: 12616152]
14. Arosarena OA, Collins WL. Bone regeneration in the rat mandible with bone morphogenetic protein-2: a comparison of two carriers. Otolaryngol Head Neck Surg 2005;132(4):592–7. [PubMed: 15806052]
15. Hu Y, Zhang C, Zhang S, Xiong Z, Xu J. Development of a porous poly(L-lactic acid)/hydroxyapatite/collagen scaffold as a BMP delivery system and its use in healing canine segmental bone defect. J Biomed Mater Res A 2003;67(2):591–8. [PubMed: 14566802]
16. Suzuki A, Terai H, Toyoda H, Namikawa T, Yokota Y, Tsunoda T, et al. A biodegradable delivery system for antibiotics and recombinant human bone morphogenetic protein-2: A potential treatment for infected bone defects. J Orthop Res 2006;24(3):327–32. [PubMed: 16479565]
17. Baltzer AW, Lattermann C, Whalen JD, Wooley P, Weiss K, Grimm M, et al. Genetic enhancement of fracture repair: healing of an experimental segmental defect by adenoviral transfer of the BMP-2 gene. Gene Ther 2000;7(9):734–9. [PubMed: 10822299]

NIH-PA Author Manuscript

NIH-PA Author Manuscript

NIH-PA Author Manuscript

18. Betz OB, Betz VM, Nazarian A, Pilapil CG, Vrahas MS, Bouxsein ML, et al. Direct percutaneous gene delivery to enhance healing of segmental bone defects. J Bone Joint Surg Am 2006;88(2):355–65. [PubMed: 16452748]
19. Lieberman JR, Daluiski A, Stevenson S, Wu L, McAllister P, Lee YP, et al. The effect of regional gene therapy with bone morphogenetic protein-2-producing bone-marrow cells on the repair of segmental femoral defects in rats. J Bone Joint Surg Am 1999;81(7):905–17. [PubMed: 10428121]
20. Xu XL, Tang T, Dai K, Zhu Z, Guo XE, Yu C, et al. Immune response and effect of adenovirus-mediated human BMP-2 gene transfer on the repair of segmental tibial bone defects in goats. Acta Orthop 2005;76(5):637–46. [PubMed: 16263609]
21. Einhorn TA, Lane JM, Burstein AH, Kopman CR, Vigorita VJ. The healing of segmental bone defects induced by demineralized bone matrix. A radiographic and biomechanical study. J Bone Joint Surg Am 1984;66(2):274–9. [PubMed: 6693455]
22. Chu, TM.; Flanagan, CL.; Hollister, S.; Feinberg, SE.; Fisher, JP.; Mikos, AG. The mechanical and in vivo performance of 3-D poly(propylene fumarate)/tricalcium phosphate scaffolds. In: Biomaterials, Sf, editor. 29th Annual meeting of Society for Biomaterials; 2003; Reno, NV: Society for Biomaterials; 2003. p. 660
23. Chu TM, Halloran JW, Hollister S, Feinberg SE. Hydroxyapatite implants with designed internal architecture. J Mater Sci: Mater Med 2001;12:471–478. [PubMed: 15348260]
24. Chu TM, Orton DG, Hollister SJ, Feinberg SE, Halloran JW. Mechanical and in vivo performance of hydroxyapatite implants with controlled architectures. Biomaterials 2002;23(5):1283–93. [PubMed: 11808536]
25. Ohura K, Hamanishi C, Tanaka S, Matsuda N. Healing of segmental bone defects in rats induced by a beta-TCP-MCPM cement combined with rhBMP-2. J Biomed Mater Res 1999;44(2):168–75. [PubMed: 10397918]
26. Yasko AW, Lane JM, Fellinger EJ, Rosen V, Wozney JM, Wang EA. The healing of segmental bone defects, induced by recombinant human bone morphogenetic protein (rhBMP-2). A radiographic, histological, and biomechanical study in rats. J Bone Joint Surg Am 1992;74(5):659–70. [PubMed: 1378056]
27. Wilson PD Jr. A clinical study of the biomechanical behavior of massive bone transplants used to reconstruct large bone defects. Clin Orthop 1972;87:81–109. [PubMed: 4562200]
28. Chmell MJ, McAndrew MP, Thomas R, Schwartz HS. Structural allografts for reconstruction of lower extremity open fractures with 10 centimeters or more of acute segmental defects. J Orthop Trauma 1995;9(3):222–6. [PubMed: 7623174]
29. Tiyapatanaputi P, Rubery PT, Carmouche J, Schwarz EM, O'Keefe RJ, Zhang X. A novel murine segmental femoral graft model. J Orthop Res 2004;22(6):1254–60. [PubMed: 15475206]
30. Chu TG, Sargent PW, Warden SJ, Turner CH, Stewart RL. Preliminary Evaluation of a Load-Bearing BMP-2 Carrier for Segmental Defect Regeneration. Biomedical Sciences Instrumentation 2006;42:42–46. [PubMed: 16817583]
31. Peter SJ, Miller ST, Zhu G, Yasko AW, Mikos AG. In vivo degradation of a poly(propylene fumarate)/beta-tricalcium phosphate injectable composite scaffold. J Biomed Mater Res 1998;41(1):1–7. [PubMed: 9641618]
32. Hyun SJ, Han DK, Choi SH, Chai JK, Cho KS, Kim CK, et al. Effect of recombinant human bone morphogenetic protein-2, -4, and -7 on bone formation in rat calvarial defects. J Periodontol 2005;76(10):1667–74. [PubMed: 16253088]

NIH-PA Author Manuscript

NIH-PA Author Manuscript

NIH-PA Author Manuscript

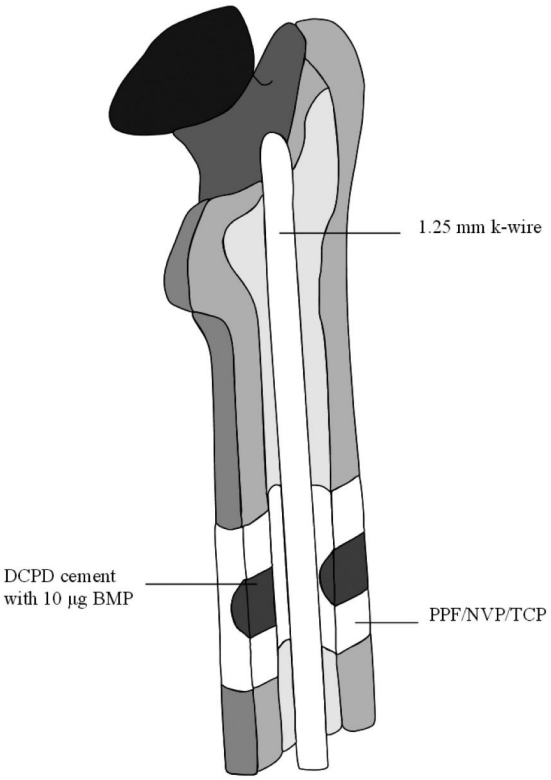

Figure 1.
Illustration of the BMP scaffold placed in rat femur segmental defect stabilized with intramedullary pin.

NIH-PA Author Manuscript

NIH-PA Author Manuscript

NIH-PA Author Manuscript

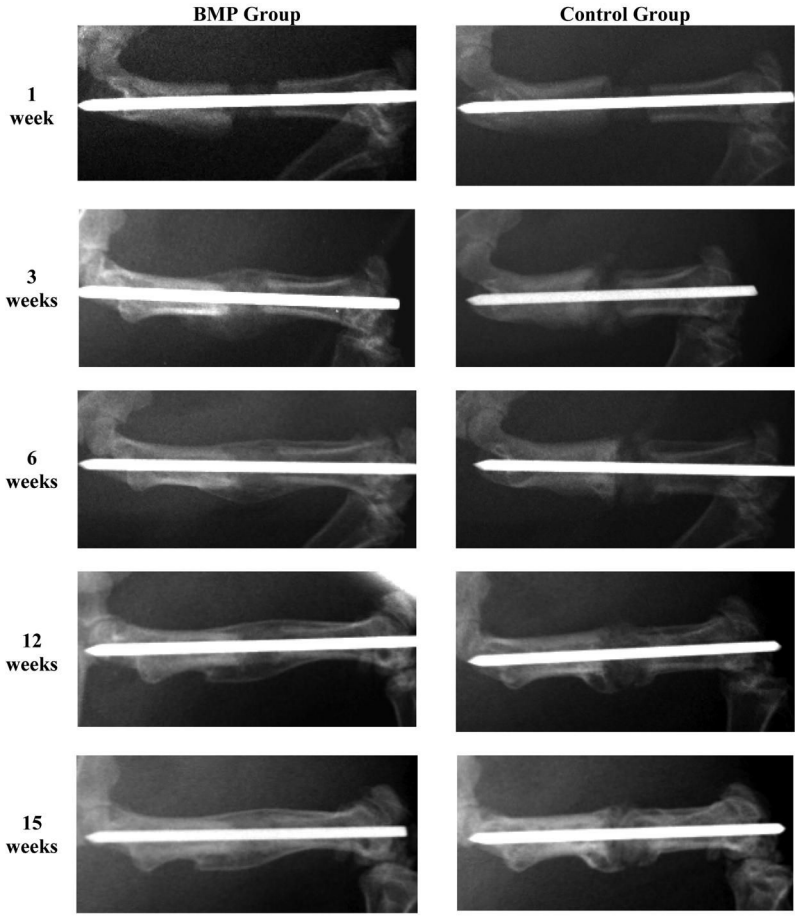

Figure 2.

Representative serial radiological images of segmental defects in the BMP and control groups at one, three, six, 12 and 15 weeks post-operatively. At three weeks, callus had formed and bridged the segmental defect in the BMP group. In the control group, some cortical bone thickening and callus formation was evident immediately adjacent to the scaffold; however, there was no bridging callus. Between six and 15 weeks, the bridging callus in the BMP group showed signs of consolidation and remodeling. In contrast, in the control group only isolated regions of radio-opacity were evident within the defect region and no bridging callus was present.

NIH-PA Author Manuscript

NIH-PA Author Manuscript

NIH-PA Author Manuscript

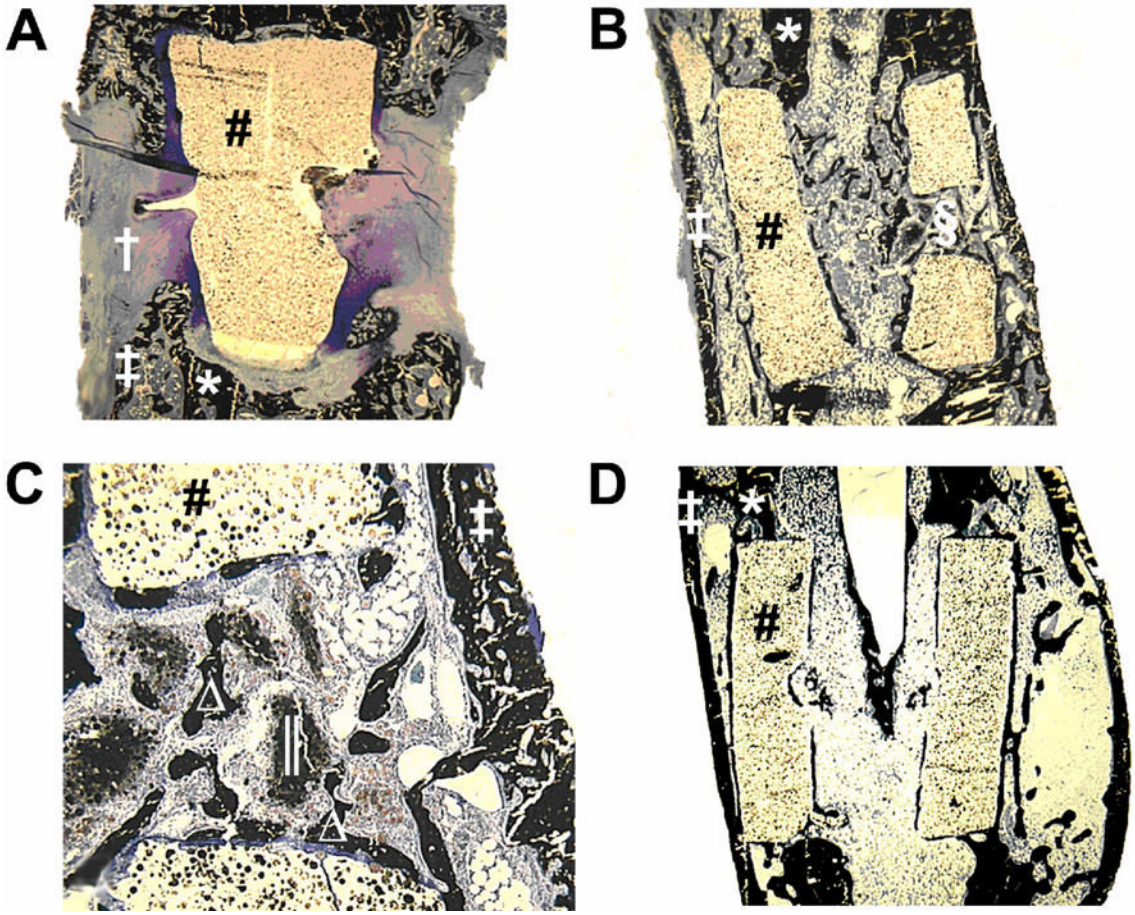

Figure 3.

Representative histological images of segmental defects in the (A) control and (B,C) rhBMP groups at six weeks post-operatively. Sections are stained with McNeal's tetrachrome, which stains bone black. (A) Segmental defects in the control group demonstrated cartilaginous union, whereas (B) defects in the BMP group were bridged by mineralized callus that (C) invaded the side hole and was on the surface of the scaffold, indicating scaffold osteoconductivity. Inflammatory cells were not present in either scaffold group. (D) By 16-weeks post-operatively in the BMP group, the osteoconductivity of the scaffold is evident by the formation of new bone on its surfaces. * = original cortex of the femoral diaphysis, # = weight bearing biodegradable scaffold, † = cartilaginous tissue, ‡ = mineralized callus, § = side hole within the scaffold, || = residual dicalcium phosphate dihydrate cement carrying rhBMP-2, Δ = mineralized callus within the side hole and on the surface of the scaffold.

NIH-PA Author Manuscript

NIH-PA Author Manuscript

NIH-PA Author Manuscript

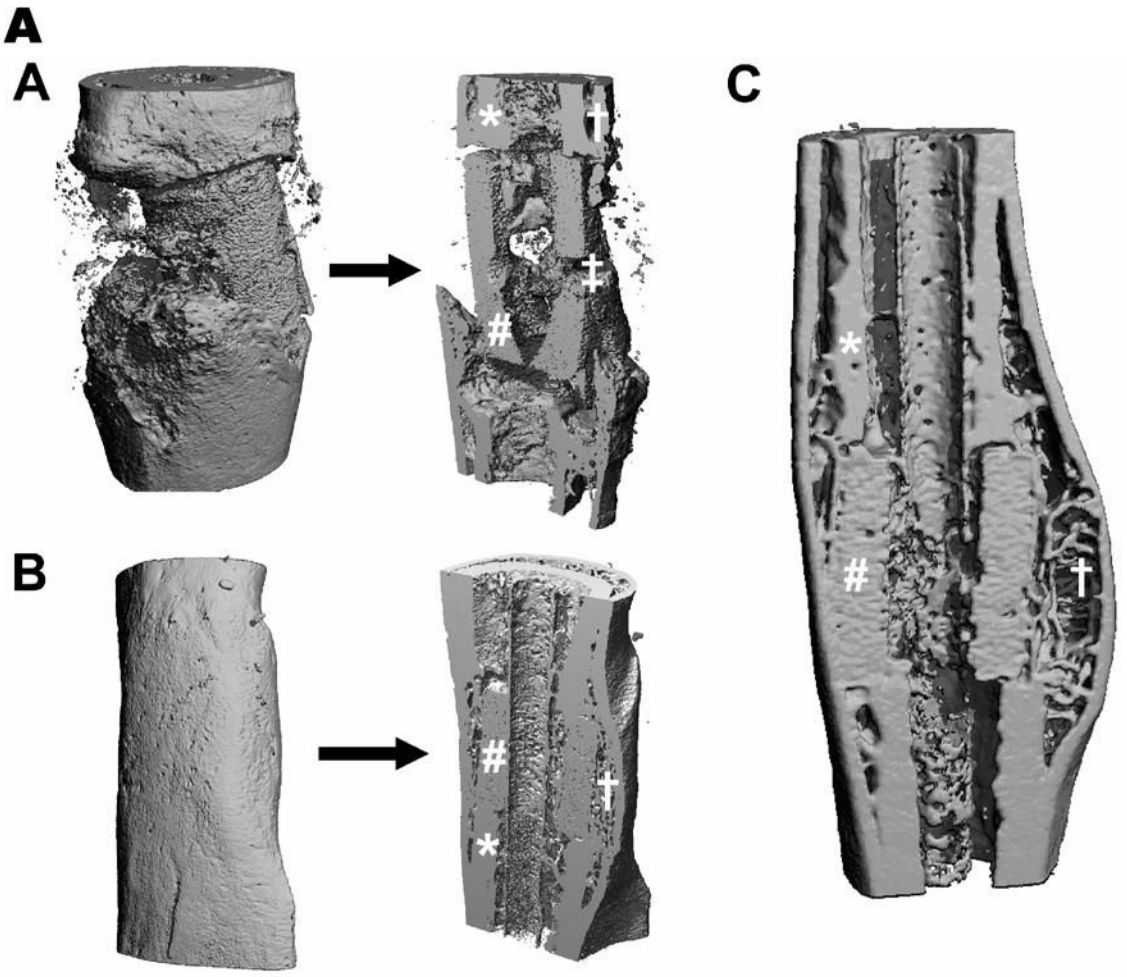

Figure 4.

Representative external and cut-away images of segmental defects in the (A) control and (B) BMP groups, as assessed by microcomputed tomography at six weeks post-operatively. (A) Segmental defects in the control group had minimal bone surrounding the scaffold and the reparative callus did not bridge the defect. (B) In contrast, the BMP group had a continuous mineralized callus around the scaffold, and bridging trabeculae beneath the cortical layer of the callus were integrated with the scaffold, indicating scaffold osteoconductivity. (C) By 16-weeks post-operatively in the BMP-group, the bridging trabeculae had thickened and there is evidence of bone formation of bone on the surfaces of the scaffold, indicating scaffold osteoconductivity. * = original cortex of the femoral diaphysis, # = weight bearing biodegradable scaffold, † = mineralized callus, ‡ = side hole within the scaffold.

NIH-PA Author Manuscript

NIH-PA Author Manuscript

NIH-PA Author Manuscript

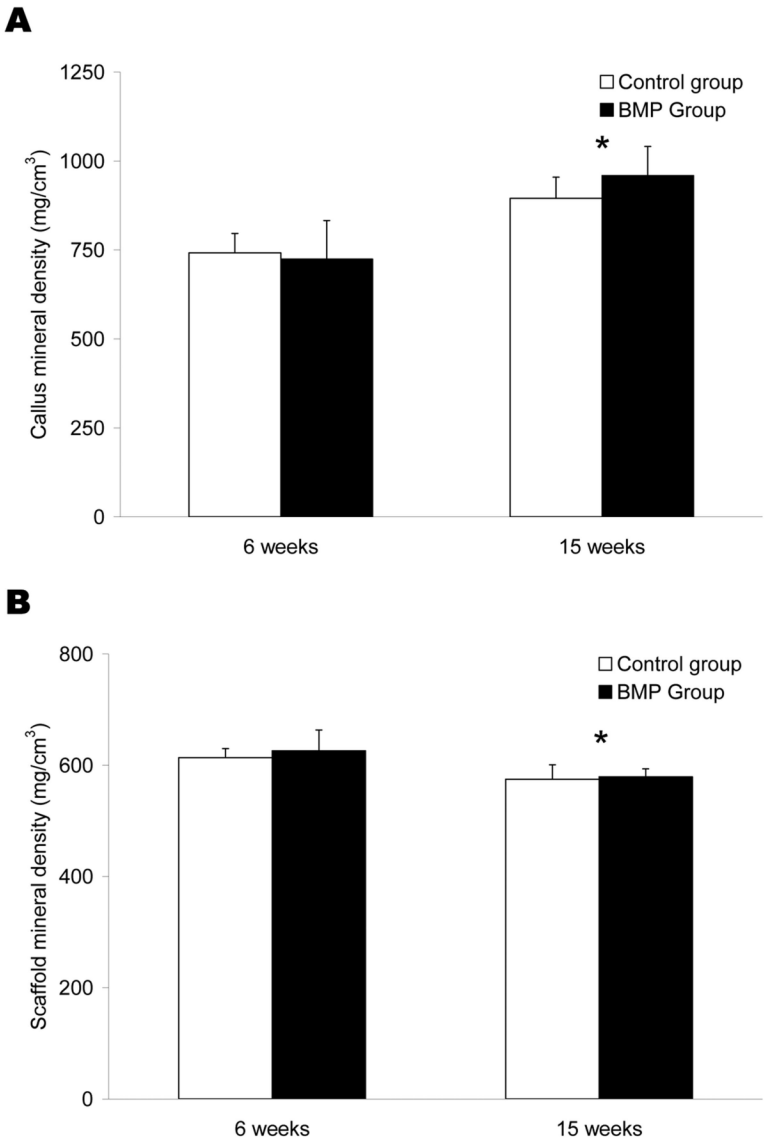

Figure 5.

Effect of scaffold group on volumetric bone mineral density (vBMD) of the: (A) callus and (B) scaffold, as assessed by peripheral quantitative computed tomography at six and 15-weeks post-operatively. * indicates significant main effect for time since surgery (six vs. 15 weeks) ($p < 0.01$).

NIH-PA Author Manuscript

NIH-PA Author Manuscript

NIH-PA Author Manuscript

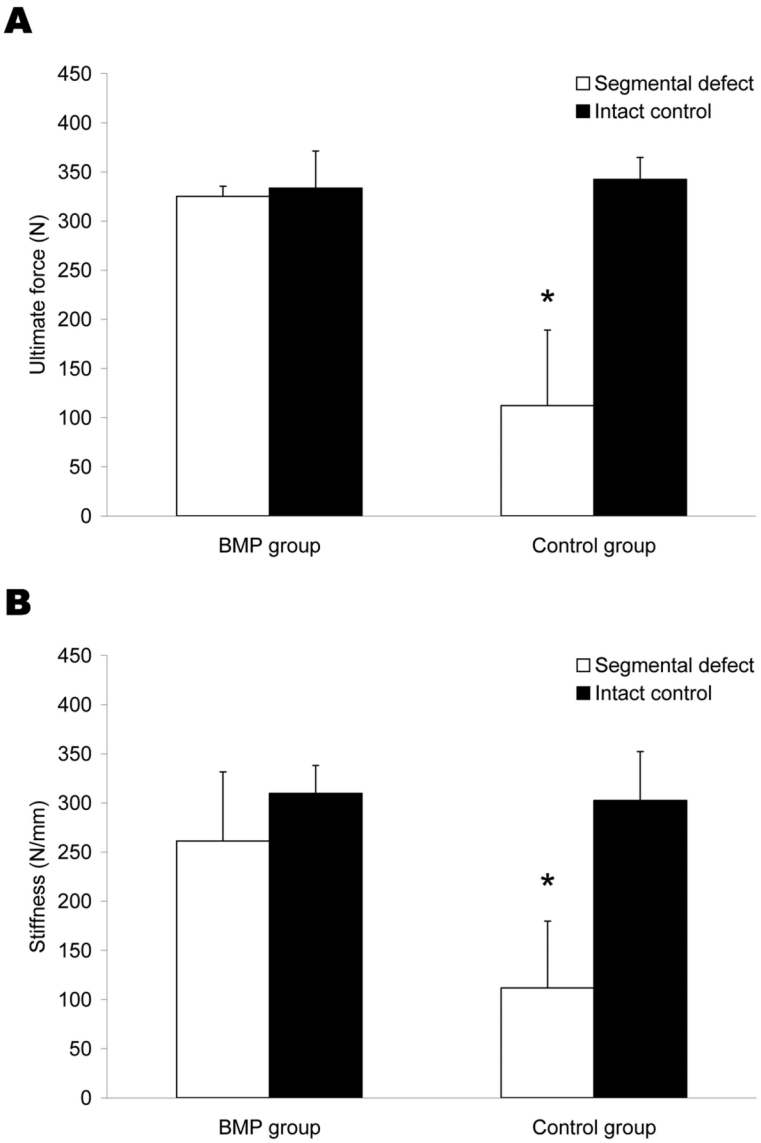

NIH-PA Author Manuscript

NIH-PA Author Manuscript

NIH-PA Author Manuscript

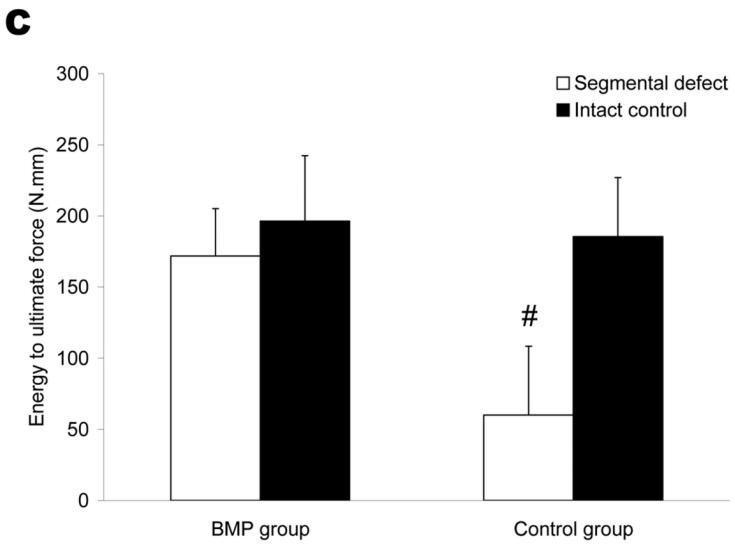

Figure 6.

Effect of scaffold group on femoral: (A) ultimate force, (B) stiffness and (C) energy to ultimate force, as assessed by mechanical testing at 15-weeks post-operatively. * indicates significantly different from all other groups ($p < 0.01$). # indicates significantly different from segmental defect in BMP group ($p = 0.02$).

NIH-PA Author Manuscript

NIH-PA Author Manuscript

NIH-PA Author Manuscript

Table 1

[[|]]	[[|]]	X-ray score		
[[|]]	**[[Week|]]**	**[[0|]]**	**[[1|]]**	**[[2|]]**
[[Control group (N=4)|]]	[[1|]]	[[4|]]	[[0|]]	[[0|]]
[[|]]	[[3|]]	[[4|]]	[[0|]]	[[0|]]
[[|]]	[[6|]]	[[4|]]	[[0|]]	[[0|]]
[[|]]	[[12|]]	[[4|]]	[[0|]]	[[0|]]
[[|]]	[[15|]]	[[3|]]	[[1|]]	[[0|]]
[[BMP group (N=4)|]]	[[1|]]	[[4|]]	[[0|]]	[[0|]]
[[|]]	[[3|]]	[[1|]]	[[1|]]	[[2|]]
[[|]]	[[6|]]	[[0|]]	[[0|]]	[[4|]]
[[|]]	[[12|]]	[[0|]]	[[0|]]	[[4|]]
[[|]]	[[15|]]	[[0|]]	[[0|]]	[[4|]]